Journal of Molecular Catalysis A: Chemical 340 (2011) 99–107

Contents lists available at ScienceDirect

Journal of Molecular Catalysis A: Chemical

journal homepage: www.elsevier.com/locate/molcata

Effect of phosphorus on novel bifunctional additives for enhancing the production of propylene and removal of SO_2 in FCC process

Xiaoling Xu, Chunyi Li*, Honghong Shan

State Key Laboratory of Heavy Oil Processing, China University of Petroleum (East China), Qingdao 266555, Shandong, China

ARTICLE INFO

Article history:
Received 13 February 2011
Received in revised form 21 March 2011
Accepted 21 March 2011
Available online 31 March 2011

Keywords:
ZSM-5
Propylene
Magnesium–aluminate spinel
SO_2 adsorption
Phosphorus

ABSTRACT

Magnesium-aluminate spinels were introduced into the matrix of typical propylene additives (ZSM-5 as the active component) to obtain a series of novel bifunctional additives for enhancing the production of propylene and removal of SO_2. Their performance as additives to a commercial equilibrium USY FCC catalyst for VGO (vacuum gas oil) cracking and activity in oxidative adsorption of SO_2 under similar FCC regenerator conditions were investigated. The bottleneck of the novel bifunctional additives is that the substitution of $MgAl_2O_4$ for Kaolin clay in propylene additives causes the migration of Mg^{2+} into ZSM-5 zeolite, which evidently lowers the activity of ZSM-5 as an FCC additive. However, pretreating $MgAl_2O_4$ with phosphoric acid either by extraction or by impregnation method which weakened the interaction between $MgAl_2O_4$ and ZSM-5 during the steaming and calcination processes, respectively, was proved to be effective in enhancing the efficiency of ZSM-5 for increasing propylene yield. Concurrently, the unusually high hydrogen transfer activity of $MgAl_2O_4$ in VGO cracking, which also contributed to the decrease in ZSM-5 activity, was sharply reduced by P doping. Moreover, the phosphorus modification also promoted the SO_2 uptake capacity of bifunctional additives.

1. Introduction

With the propylene demand continuously growing in recent years, fluid catalytic cracking (FCC) process has made efforts both on process and catalyst side as a major source of incremental propylene. The addition of ZSM-5 containing additives to FCC catalysts is one of the effective means for improving propylene yield [1–14]. It has been found that the performance of ZSM-5 as an FCC catalyst additive in improving propylene yield is dependent on many factors. For example, it has been proposed that combining ZSM-5 addition with high severity operation would be an attractive option for increasing light olefins [9]. Triantafillidis and Evmiridis have investigated the effects of the total ZSM-5 acidity and the size of ZSM-5 particles on LPG increase [2]. Besides, an important proposition that has been proved is that the effectiveness of ZSM-5 decreases with increasing the hydrogen transfer activity of the base catalyst or increasing naphthenes in the feed [5,12]. Wallenstein and Harding have demonstrated that gasoline olefinicity is the dominant contributor to ZSM-5 performance by testing with REUSY catalysts of different rare-earth contents and different feeds [3]. Apart from the above factors, a suitable matrix is also an important parameter affecting performance of these propylene additives. To make better use of ZSM-5, inert matrices such as clays and silica and/or alumina binder are generally used in typical propylene additives [2,7].

On the other hand, the removal of SO*x* from FCC units has been the subject of a considerable amount of attention over the past few years. To date, the least costly means is the use of a so-called sulfur-transfer technique, which is to mix the FCC catalyst with sulfur-transfer agent. The sulfur-transfer agent can fix SO*x* as a sulfate in the regenerator under oxidation atmosphere [15–24]. Since 1980s, magnesium-aluminate spinel materials have been commercially used as sulfur-transfer agent in FCC units for reduction of SO*x* emission [15–22]. Considering the high melting point (2135 °C), chemical inertness and good thermal stability of $MgAl_2O_4$ [25–28] as well as the fact that the matrix of a typical propylene additive is basically inert, an assumption of incorporating magnesium-aluminate spinel into the matrix of a propylene additive was put forward. It should be noted that some rare earth metal oxides and/or transtion metal oxides are usually introduced into $MgAl_2O_4$ to improve the De-SO*x* activity in practice [15,17,18,21]. But for convenience of investigation, only $MgAl_2O_4$ was employed to simplify the study system.

In our study, attempts were made to introduce $MgAl_2O_4$ as partial matrix of propylene additives, expecting to achieve dual functions in FCC units, i.e. maximization of propylene yield and removal of SO_2. In this way the synthesis of bifunctional additives which combine the two functions in a single particle can greatly cut the cost down and attach the significance of environmental protection with economic benefits.

* Corresponding author. Tel.: +86 532 86981862.
E-mail addresses: muzixxl@163.com (X. Xu), chyli@upc.edu.cn (C. Li).

1381-1169/$ – see front matter © 2011 Elsevier B.V. All rights reserved.
doi:10.1016/j.molcata.2011.03.014

Previously we have investigated the performance of the bifunctional additives including $MgAl_2O_4$ prepared via citrate–nitrate route [29]. It was clarified that the existence of magnesium though in the form of stable spinel would interact with ZSM-5 during calcination and severe hydrothermal conditions, resulting in lower ZSM-5 activity. There the negative effect was counteracted by modifying ZSM-5 with La and P. However, the $MgAl_2O_4$ prepared via citrate-nitrate route had a very low surface area (20.9 m^2/g) which was not favorable to the adsorption of SO_2. In this paper, $MgAl_2O_4$ was prepared by acidic sol–gel method in order to obtain spinels with a relatively large surface area. It should be expected that the bifunctional additive containing $MgAl_2O_4$ thus prepared is also less active in increasing propylene yield. In the present work, some measures were taken on the side of $MgAl_2O_4$ to improve the activity of ZSM-5.

It has been reported that the surface of $MgAl_2O_4$ powder could be passivated against hydrolysis with H_3PO_4 and $Al(H_2PO_4)_3$ solution [30]. The monolayer coverage of phosphate formed on the surface of $MgAl_2O_4$ particle could effectively protect the powder from reacting with water. Thus the modification of $MgAl_2O_4$ with phosphorus was adopted, expecting that the formed phosphate layer could inhibit the hydrolysis of spinel and weaken the interaction of spinel with ZSM-5 under hydrothermal conditions. The results showed that the modification of $MgAl_2O_4$ with P was effective in promoting both ZSM-5 activity and SO_2 uptake capacity for bifunctional additives.

It should be pointed out that the introduction of P was supposed to indirectly affect the ZSM-5 zeolite by modulating the interaction between $MgAl_2O_4$ and ZSM-5 via modification of the spinel surface. With the aim of analyzing the effect of P on the interaction, the zeolites which were separated after premixing with spinels and undergoing the calcination and steaming processes were characterized by XRD, NMR and XRF methods. Simultaneously, the P species which were initially anchored on the spinel surface could also diffuse into the ZSM-5 zeolites and modify the ZSM-5 acidity during the calcination and steaming processes. As regards this effect, many studies in the literature have already verified that P doping induces a stabilization of ZSM-5 framework during the steaming treatment [31–38]. Moreover, the catalytic properties of spinels would probably be changed with P modification which may in turn have an impact on the catalytic behavior of ZSM-5. To the best of our knowledge, few previous papers have addressed toward the effect of matrices in propylene additives on the ZSM-5 efficiency in improving propylene yield. On the whole, the role of P on the catalytic performance of bifunctional additives for improving propylene yield is more complicated and worthy of further exploration.

2. Experimental

2.1. Preparation of catalysts

$MgAl_2O_4$ was prepared by sol–gel method as follows [39]: pseudo-boehmite powder was suspended in distilled water in a vessel, and then a suitable amount of HCl solution was added dropwise under vigorous stirring at 80 °C until the pH value fell into the range of 3–4. The magnesium nitrate solution was prepared by dissolving the desired amounts of metal nitrate in the distilled water. Then the nitrate solution was added slowly into the pseudo-boehmite gel under vigorous stirring for a further 2 h. The gel obtained was then dried at 120 °C overnight. Finally they were calcined at 800 °C for 4 h.

The formula of a novel bifunctional additive which is denoted as M was: 30 wt% of HZSM-5, 6 wt% of SiO_2 (silica sol as binder), 20 wt% of $MgAl_2O_4$ and 44 wt% of Kaolin clay. And a typical propylene additive containing 30 wt% of HZSM-5 and 6 wt% of SiO_2 and 64 wt% of Kaolin clay was used as a reference and labeled as K.

Moreover, two methods were employed to modify the surface of magnesium-aluminate spinel. One was mixing the suspension of $MgAl_2O_4$ powder with a dilute solution of phosphoric acid at 70 °C for 4 h. Then the suspension was filtered and dried. The extraction procedure was repeated twice. Afterwards the obtained solid was calcined at 700 °C. The other was the impregnation method, which invovled impregnating 12.5% of P_2O_5 on the surface of $MgAl_2O_4$ powder followed by calcinating at 700 °C. The spinels modified by extraction and impregnation methods were denoted as $MgAl_2O_4$-P1 and $MgAl_2O_4$-P2, respectively. Then the treated $MgAl_2O_4$ powder was added into the matrix of propylene additive with the same concentration as that of M based on the anhydrous weight of pure $MgAl_2O_4$. The prepared bifunctional additives containing $MgAl_2O_4$-P1 and $MgAl_2O_4$-P2 were marked as M-P1 and M-P2, respectively. The obtained fresh M-P1 was further ion exchanged with NH_4Cl solution twice at 80 °C for 2 h, which was marked as M-P1-i.e.

The additives were all hydrothermally treated at 800 °C under a 100% steam flow for 4 h before catalytic evaluation.

For verifying the interaction between $MgAl_2O_4$ and ZSM-5 zeolite during the calcination and steaming processes, the ZSM-5 zeolite and parent and P-modified $MgAl_2O_4$ powder of different particle sizes (smaller than 0.054 mm for ZSM-5 zeolite and 0.106–0.2 mm for spinel powder, w(ZSM-5)/w($MgAl_2O_4$) = 3/2) were physically mixed and treated under two conditions: one was obtained by calcining the mixture at 700 °C for 2 h after being placed in the moisture air for 24 h; the other was treating the above calcined mixture at the same hydrothermal condition as mentioned above. The particles of ZSM-5 zeolites smaller than 0.054 mm were obtained by screening the mixture. The resulting ZSM-5 zeolites after the above treatments were reckoned as the fresh and aged zeolites, respectively. The ZSM-5 zeolites premixing with $MgAl_2O_4$, $MgAl_2O_4$-P1 and $MgAl_2O_4$-P2 were labeled as ZSM-5-M, ZSM-5-MP1 and ZSM-5-MP2, respectively. The compositions of these zeolites were characterized by XRF.

2.2. Evaluation of additives

The experiments concerning catalytic cracking performance were carried out in a fixed microreactor unit based on ASTM D 3907-80. The feedstock was preheated before injecting into the stainless steel reactor. The products were quenched using ice bath and separated into liquid and gas products. After injecting the feedstock, the catalyst bed and the gas products were purged with a stream of 30 ml/min N_2 for 600 s to a total gas volume that was determined by the amount of displaced water. The mass of feedstock was 1 g and the oil was injected for 75 s. All MAT runs were performed at a temperature of 540 °C and a C/O ratio of 6. The feedstock used in the tests was Daqing VGO.

The FCC catalyst ZC-7300 (marked as B) which comprises USY zeolites as active components was employed as the base catalyst to evaluate the catalytic performance of propylene additives. Catalytic performance was evaluated for the USY catalyst and USY catalyst/ZSM-5 mixtures with VGO feed on MAT units.

The properties of ZC-7300 catalyst and Daqing VGO feedstock were described earlier in reference [29].

The compositions of gaseous products were analyzed by a Varian 3800 Gas Chromatograph (GC) with a FID detector coupled with an Al_2O_3 PLOT capillary column. The liquid products were examined using a simulated distillations gas chromatogram as described by the ASTM D2887 standard to obtain the percentage weight of gasoline, diesel oil (LCO) and heavy oil (HCO). The amount of coke deposited on the catalysts after cracking was determined by ana-

lyzing the amount of CO_2 obtained from the burning of coke in situ using the chromatogram.

The SO*x* uptake tests were made on a self-assembled apparatus as in reference [22]. The SO_2 concentration of gases at different reaction time was detected by a flue gas analyser Testo 350EPA. The typical composition of flow gas before reaction was: 0.3 vol% of SO_2, 17.86 vol% of O_2, and N_2 as the balance. The temperature of SO_2 adsorption was settled at 700 °C. The evaluation for SO_2 removal of each additive was repeated for three times.

2.3. Characterization

XRD was performed using the X'Pert PRO MPD (DANalytical Co.) diffractometer with Cu-Kα radiation (45 kV, 40 mA).

BET surface area was measured by nitrogen adsorption at −196 °C using the TRIS-TAR3000 porosimeter made by Micromeritics Co. The pore size distribution was calculated from the desorption branches of the isotherms using BJH method.

The acidity of samples and the FT-IR spectra of the spinels were recorded using a Nexus Model Infrared Spectrophotometer. The acidity was measured by pyridine adsorption. First the samples were evacuated in situ in an IR cell at 300 °C for 4 h. After the temperature decreased to room temperature, the IR spectra were then recorded. Next pyridine was introduced into the cell and allowed to saturate the sample surface for 4 h. Finally, the FT-IR spectra were taken at 200 °C and 350 °C respectively to discover the relative amount of acid sites with different strength. The FT-IR spectra were measured at room temperature with a normal resolution of 4 cm^{-1} and averaging 64 spectra. Prior to analysis, thin cylinders (diameter ~1 cm) were prepared by uniaxial pressing a powder mixture of sample powder with KBr.

Acid amounts of the aged zeolites were measured by temperature-programmed desorption of ammonia (NH_3-TPD) method. 0.1 g samples with 20–60 mesh were pretreated in helium at 500 °C for 2 h, cooled to100 °C and adsorbed NH_3 for 45 min. After flushing by pure helium gas at 100 °C for 1 h, temperature-programmed desorption was started at a heating rate of 10 °C/min from 100 °C to 600 °C, and the signal was monitored with a TCD.

Nuclear magnetic resonance (NMR) experiments were carried out on a Brucker Advance III 400 equipped with a 4 mm magic angle spinning probe. ^{27}Al NMR was carried out with $Al(H_2O)_6^{3+}$ as the reference at 104.0 MHz, with the pulse of 0.3 μs (π/20°), 5000 transients separated by a 0.3 s delay.

3. Results and discussion

3.1. Performance of ZSM-5 containing additives for VGO cracking

3.1.1. The comparison of the bifunctional additive M with the typical propylene additive K

MAT tests were carried out for the cracking of VGO over the base catalyst and catalyst mixtures (10 wt% of propylene additives + 90 wt% of ZC-7300).

As seen from Fig. 1(a) and (b), the addition of the typical propylene additive K brought slight increases in the yields of ethylene and dry gas and distinct increases in LPG and propylene and butylene yields. But for the additive M, the replacement of 20% Kaolin clay by $MgAl_2O_4$ lowered the efficiency of ZSM-5, obviously reducing the incremental yields of propylene and butylene. Concurrently, the yields of ethylene and dry gas were practically unchanged with the addition of M. This should be ascribed to the ion exchange between Mg^{2+} and zeolite as clarified earlier [29].

Fig. 1(c) shows that the loss in gasoline yield was much higher for K than that for M. It should be mentioned that the addition of M boosted the LCO yield compared to the base catalyst, while the

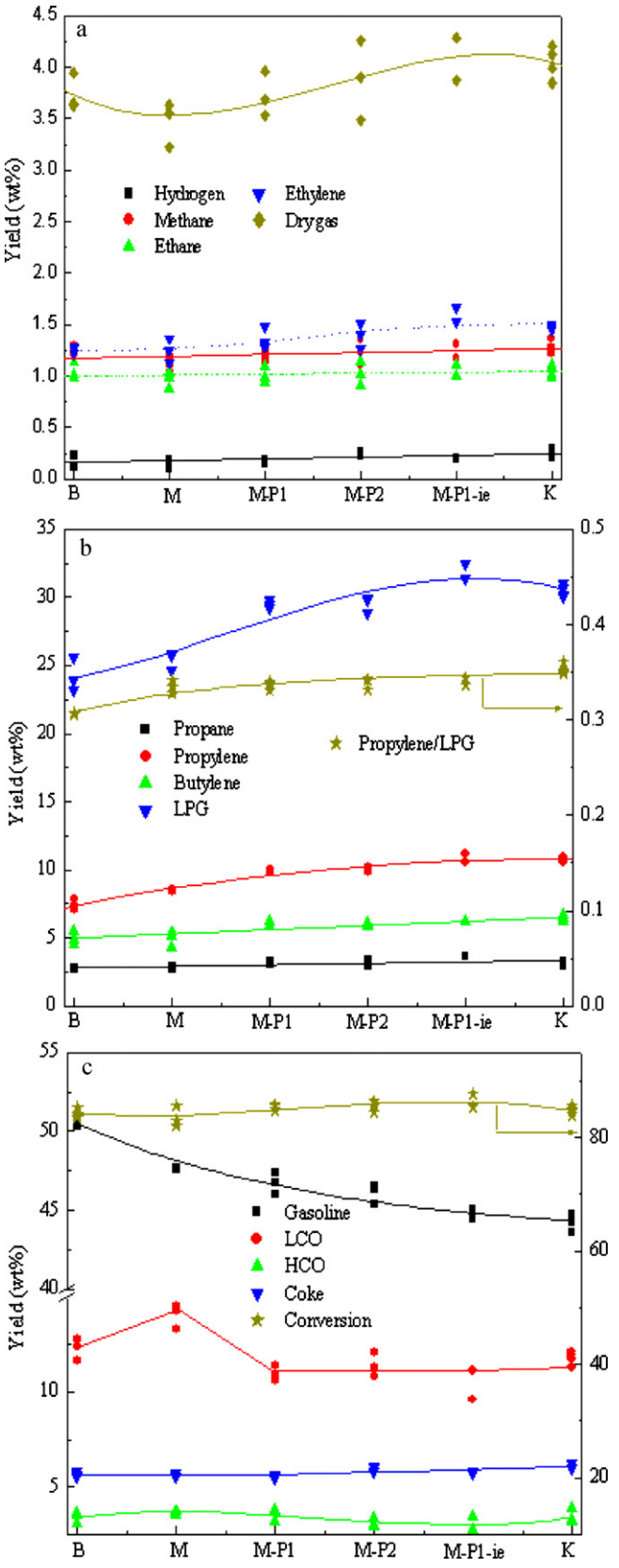

Fig. 1. Compositions of dry gas (a), LPG (b) and liquid products (c) over USY or mixtures of USY and different aged additives. (The letters M, M-P1, M-P2, M-P1-i.e. are indicative of mixtures of B and corresponding additives.).

yield dropped with the addition of K. It has been proved in RIPP's laboratory that higher LCO yield can be achieved by introducing alkaline earth metal oxides into the zeolite component [40]. Hence it should be proposed that some interaction of $MgAl_2O_4$ with ZSM-5 zeolite was present in the additive M. Besides, the introduction of the two additives caused minor influence on the conversion and the yields of HCO and coke.

3.1.2. Effect of P on the catalytic performance of bifunctional additives

Since the activity of ZSM-5 for improving propylene yield was lowered by introducing $MgAl_2O_4$ into the matrix, the orientation was focused on modifying $MgAl_2O_4$ with P in order to reduce the interaction between $MgAl_2O_4$ and ZSM-5.

The results with the two additives M-P1 and M-P2 showed that the ethylene, propylene, butylene and LPG yields were clearly enhanced after treating $MgAl_2O_4$ with phosphoric acid, implying improved ZSM-5 activity in both M-P1 and M-P2. But the change on the propylene selectivity in LPG can be hardly observed. Besides, the incremental yields of light olefins (C_2-C_4) were still lower than those with the addition of K. The possibility may be that some Mg^{2+} ions were still remained free to enter the pores of the zeolite.

For checking out whether migratory Mg^{2+} ions were present in the additive M-P1, the additive M-P1-i.e. prepared by exchanging the fresh M-P1 with ammonium ions was also tested. It can be found that the yields of light olefins and LPG were further enhanced in comparison with M-P1. Moreover, those yields for the additive M-P1-i.e. were comparable to those for the additive K that is free of $MgAl_2O_4$, suggesting that the migratory Mg^{2+} remained in the additive M-P1 can be further removed through ion exchange process.

The variation in gasoline yield was consistent with that of LPG yield. In general, the more loss in gasoline yield, the more gain in LPG yield. Concerning the LCO yield, much different from the case of M, the yield dropped for all bifunctional additives containing P. It may indicate that the interaction of $MgAl_2O_4$ with ZSM-5 zeolite was attenuated by the presence of P. Similarly, the conversion and coke yield changed little with their addition.

3.2. The SO_2 adsorption activity of the bifunctional additives

As expected, it can be observed (Fig. 2) that all of the bifunctional additives containing $MgAl_2O_4$ revealed notable capacity in adsorption of SO_2. Evidently, the additives containing P (M-P1 and M-P2) had higher activity and stability in adsorption of SO_2 than the additive M. When comparing the SO_2 adsorption activity of M-P1 with M-P2, it can be inferred that the acitivity was lower for the additive with higher P content. Nevertheless, the capacity of SO_2 oxidative adsorption was declined and became close to that of M when the additive M-P1 was further ion exchanged with NH_4^+ obtaining M-P1-i.e.

In summary, it should be identified that the modification of $MgAl_2O_4$ with P either by extraction or impregnation method could significantly enhance the SO_2 pick-up activity of the bifunctional additives. But the additional ion exchange process was unfavorable to the uptake of SO_2.

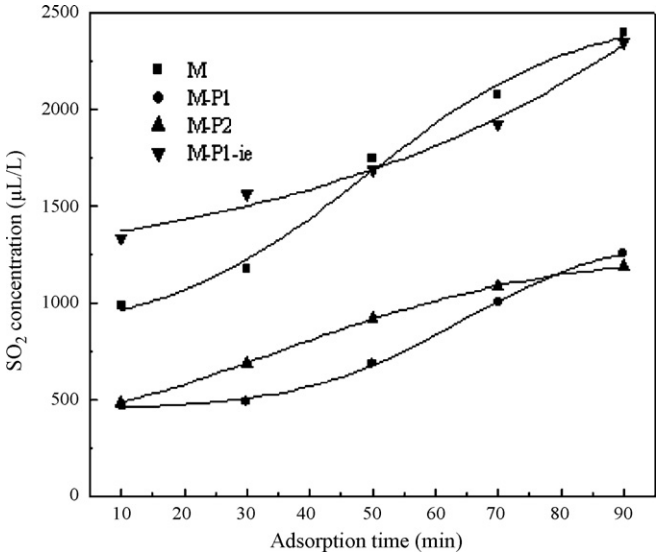

Fig. 2. The adsorption activity of SO_2 over different novel bifunctional additives.

3.3. Effect of P on the structure of the zeolites interacting with $MgAl_2O_4$

On the basis of the XRD patterns for the zeolites, the sum of the reflection intensities at 2θ of 23.1°, 23.3°, 23.9° and 24.3° for the other zeolites divided by the sum of these peak intensities for the fresh ZSM-5 was referred to as the relative crystallinity.

With regard to the fresh samples, ZSM-5-M presented relative crystallinity of 96.8%, indicating that the interaction of ZSM-5 with $MgAl_2O_4$ had little effect on the zeolite structure. This was consistent with the previous result that the structure and crystallinity of the zeolites were not much changed after the solid-state reaction of ZSM-5 with $MgC1_2$ [41]. A similar conclusion was made in the case of solid-state exchange of ZSM-5 with In^{3+} [42]. They both attributed this behavior to the high thermal and chemical stability of ZSM-5 zeolite. On the other hand, the relative crystallinity of ZSM-5-MP1 and ZSM-5-MP2 were 93.2% and 95.6%, respectively. It may be explained by the interaction of P with ZSM-5, in accordance with the effect of P modification on the ZSM-5 zeolite [31–33].

After hydrothermal treatment, the crystallinity of ZSM-5 zeolite for all samples was greatly decreased. Relative to the crystallinity of 79.8% for the aged ZSM-5, the aged ZSM-5-M had lower crystallinity of 73.8%. However, slightly higher crystallinity of 74.6% and 76.0% were obtained for the aged ZSM-5-MP1 and ZSM-5-MP2, respectively.

For comparison, the ZSM-5 zeolites with different contents of Mg by direct impregnation method were also prepared. The samples were identified as "ZSM-5" followed by the Mg content, expressed in wt%. The crystallinity of these fresh and aged zeolites was shown in Table 1. Whether for the fresh zeolites or the aged ones, the ZSM-5 crystallinity decreased with increasing Mg content. And the preservation of the crystallinity during steaming was lower in the case of higher Mg content. Since the Mg content that entered the zeolite during the interaction between ZSM-5 and $MgAl_2O_4$ was less than 0.1% (Table 2), it should be reasonable to

Table 1
The crystallinity of the ZSM-5 zeolites by direct impregnation with different contents of Mg.

Sample	ZSM-5	ZSM-5-0.5Mg	ZSM-5-1Mg	ZSM-5-2.5Mg
ZSM-5 crystallinity (%)				
Fresh	100	91.8	88.0	85.6
Aged	79.8	70.5	65.4	57.2

Table 2
The compositions of the zeolites interacting with $MgAl_2O_4$ determined by XRF.

Sample	Content (wt%)				
	Mg	Al	Si	O	P
ZSM-5 fresh	–	2.768	44.084	52.814	–
ZSM-5-M fresh	0.040	2.716	43.999	52.759	–
ZSM-5-M aged	0.078	2.803	43.829	52.696	–
ZSM-5-MP1 fresh	0.062	2.759	43.974	52.776	0.015
ZSM-5-MP1 aged	0.074	2.797	43.846	52.732	0.039
ZSM-5-MP2 fresh	0.026	2.730	44.007	52.769	0.010
ZSM-5-MP2 aged	0.061	2.803	43.867	52.749	0.039

deduce that the structure of zeolite was scarcely damaged by the interaction either during the calcination or steaming process. And this was well confirmed by the former XRD results.

To make clear the role of P in modulating the interaction between $MgAl_2O_4$ and ZSM-5, the ^{27}Al MAS NMR spectra (Fig. 3) were shown to illustrate the framework of the zeolites.

The spectrum of the fresh ZSM-5 consisted of an intense signal at 54 ppm assigned to the framework tetrahedral Al and a much weaker signal at about 0 ppm typical of extra-framework octahedral aluminum. As shown in the spectrum of ZSM-5-M, the signal of tetrahedral Al in the framework (54 ppm) decreased appreciably after the ZSM-5 zeolites were contacted with $MgAl_2O_4$ materials. Moreover, the fresh ZSM-5-MP1 and ZSM-5-MP2 exhibited very similar spectra to that of ZSM-5-M.

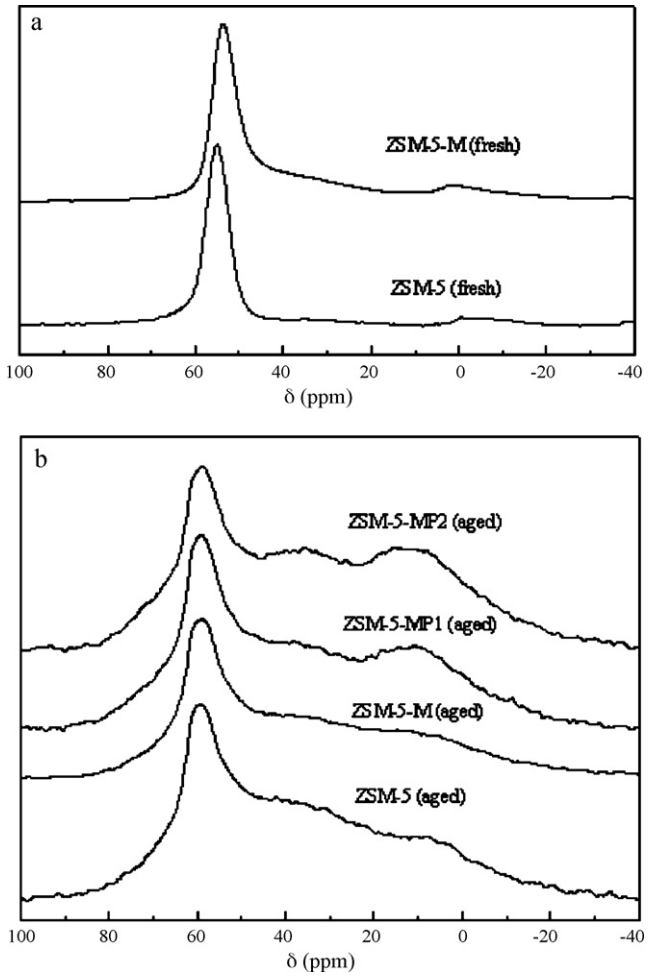

Fig. 3. ^{27}Al MAS NMR spectra of the zeolites: (a) fresh ZSM-5 and ZSM-5-M, (b) aged ZSM-5, ZSM-5-M, ZSM-5-MP1 and ZSM-5-MP2.

After steaming, as expected, all of the samples exhibited significant decreases for the signal at 54 ppm and increases for the signal at 0 ppm, identifying the dealumination process during the hydrothermal treatment. The spectra displayed that the intensity of tetrahedral Al for the aged ZSM-5-M was mildly lower than that of the aged ZSM-5. Furthermore, the corresponding zeolites obtained by contacting with P-modified $MgAl_2O_4$ did not exhibit improved intensity at 54 ppm.

The band in the intermediate region of 46–13 ppm related to the intermediate Al species existed in all the steamed samples. However, its assignment remains controversial. Menezes and coworkers [34,35] proposed that the intermediate species could be divided into two types: one at 45–36 ppm could be attributed to tetrahedral Al in a distorted environment; the other intermediate species at 30–13 ppm were more likely to be correlated with the pentacoordinated species attached to P. But these intermediate species cannot be unambiguously assigned by the common ^{27}Al MAS NMR spectra. The signal at 40–30 ppm has also been attributed to tetrahedral Al in an extra-framework aluminum phosphate or the formation of $(SiO)_xAl(OP)_{4-x}$ sites by substitution of some P by Si atoms [32,36,37]. Here the intermediate species at 46–13 ppm were not further divided. And it can be observed that the proportion of these intermediate species was especially higher for the aged ZSM-5-MP1 and ZSM-5-MP2. In addition, the proportion of the intermediate Al was the largest when P was introduced by impregnation.

The amounts of P in the aged samples ZSM-5-MP1 and ZSM-5-MP2 were approximately the same as determined by XRF (Table 2), although $MgAl_2O_4$-P1 and $MgAl_2O_4$-P2 contained 9.15% and 12.48% of P_2O_5, respectively. It could be concluded that this minor amount of P in the zeolites greatly increased the amount of the intermediate Al species, which can also contribute to the zeolite acidity [34,38].

The XRF results (Table 2) showed that the mixing of $MgAl_2O_4$ with ZSM-5 at high calcination temperature caused the integration of Mg into the ZSM-5 zeolite. Meanwhile, when the mixture of $MgAl_2O_4$ and ZSM-5 first calcined at 700 °C was then steamed at 800 °C, the concentration of Mg in the ZSM-5 zeolite was further increased. This indicated that the hydrothermal treatment further promoted the interaction between $MgAl_2O_4$ and ZSM-5. As to the role of P, the higher Mg content of the fresh zeolite ZSM-5-MP1 than the fresh ZSM-5-M and the approximately equal Mg content for both aged zeolites demonstrated that extracting $MgAl_2O_4$ with phosphoric acid was more effective in suppression of the interaction between ZSM-5 zeolite and $MgAl_2O_4$ during steaming. But the lower Mg content of the fresh ZSM-5-MP2 than the fresh ZSM-5-M suggested that the impregnation method was more helpful in restraining the interaction during calcination.

As presumed by Sulikowski et al. [43], some oxides could diffuse into the pores of the zeolite lattice when the mixtures of zeolite and oxides are calcined within certain temperature and composition ranges. However, for oxides with extremely high melting point and low solubility in hot water, the presence of small amounts of water (vapor) may be even an indispensable prerequisite for the occurance of solid-state interaction between zeolite and oxides. In

Table 3
Amount of B and L acid sites determined by FTIR of pyridine adsorption for the fresh zeolites and additives at different desorption temperatures.

Sample	Total acidity (μmol g^{-1}) (200 °C)			Strong acidity (μmol g^{-1}) (350 °C)		
	B	L	L/B	B	L	L/B
ZSM-5	633.39	90.03	0.14	568.22	38.05	0.07
ZSM-5-M	334.91	118.02	0.35	323.46	42.92	0.13
ZSM-5-MP1	318.68	79.68	0.25	302.26	25.67	0.08
ZSM-5-MP2	366.65	86.57	0.24	340.47	32.60	0.10
K	140.67	55.40	0.39	128.55	25.35	0.20
M	55.80	22.11	0.40	55.35	12.12	0.22
M-P1	53.85	47.00	0.87	50.32	24.30	0.48
M-P2	97.19	45.03	0.46	89.99	28.17	0.31

view of the properties of $MgAl_2O_4$, such as extremely high melting point and hydrophobic character [44], the solid-state ion exchange between ZSM-5 zeolite and $MgAl_2O_4$ would be highly difficlut to occur. Nevertheless, the XRF and the acidity (as disscussed in Section 3.4) results indicated that $MgAl_2O_4$ could be transported into the zeolite and substituted for some acidic sites of ZSM-5 during calcination. This may be correlated with the purity of spinel prepared here. It should be reminded that not all of Mg and Al atoms were transformed into the spinel phase and some amorphous phases were present. During steaming, i.e., in the presence of water vapor and high temperature, the solid-state interaction between ZSM-5 and $MgAl_2O_4$ would be further reinforced.

3.4. Effect of P on the acidity of zeolites and additives

Infrared spectra using pyridine as probe molecule are widely adopted to probe the surface acidity of zeolites. The band around 1540 cm^{-1} is assumed to be characteristic for pyridinium ions (Brønsted acid sites), while the band at about 1450 cm^{-1} is attributed to coordinatively adsorbed pyridine (Lewis acid sites) [45]. The adsorption amount of pyridine degassed at the temperature of 200 °C corresponds to the total acid amount, while the adsorption amount of pyridine degassed at relatively higher temperature of 350 °C represents the acid amount of strong strength. The acidity of the ZSM-5 zeolites and additives before and after steaming was characterized by FTIR of pyridine adsorption after desorption at 200 °C and 350 °C, respectively. The acid amounts of fresh and aged samples determined by FTIR of pyridine adsorption were summarized in Tables 3 and 4, respectively.

As observed in Table 3, the total and strong Brønsted acidity of ZSM-5-M showed remarkable decreases relative to those of ZSM-5, whereas the amount of Lewis acid sites and L/B ratio were increased as $MgAl_2O_4$ was contacted with ZSM-5. But almost all of the changes in the acidity caused by the interaction between $MgAl_2O_4$ and ZSM-5 were retarded with the introduction of P (especially for ZSM-5-MP2), except that the Brønsted acidity of ZSM-5-MP1 was even lower than ZSM-5-M. The exception may probably be related to the higher Mg content in the fresh ZSM-5-MP1 than fresh ZSM-5-M.

The Brønsted acidity of different additives changed similarly to that of zeolites. However, the variation in Lewis acidity of the additives was quite different from that of zeolites. Concerning the zeolites, the Lewis acidity for ZSM-5-M was higher than ZSM-5 and the weak acid sites dominated in the increased Lewis acidity, which was in line with previous results when Mg^{2+} was incorporated into ZSM-5 by solid-state reaction [41]. While the contrary changes in Lewis acidity for the additives may be explained in the aspect of matrix, such as the different acidity of Kaolin clay and $MgAl_2O_4$.

As for the aged samples (Table 4), ZSM-5-M showed obviously lower Brønsted acidity and higher Lewis acidity and a much larger value in the ratio of weak acid sites/strong acid sites than those of ZSM-5. The Brønsted acid sites for the two zeolites interacting with P-modified $MgAl_2O_4$ were only slightly larger than that of ZSM-5-M. But the ratio of weak acid sites/strong acid sites was evidently reduced with the incorporation of P. Likewise, the variation in Brønsted acidity for the additives was similar to that of the zeolites despite the large difference for the changes in strong Lewis acidity. As for the zeolites, the strong Lewis acid amount decreased due to the interaction with $MgAl_2O_4$ but increased by P doping, whereas the opposite trend was found for the additives.

Previous literature has demonstrated that the Brønsted acidity of the aged ZSM-5 samples could be obviously improved by P modification [36,38]. However, it should be stressing that P indirectly interacted with the ZSM-5 zeolite in this case, resulting in a minor amount of P in the zeolite and not so pronounced effect in improving the hydrothermal stability of the zeolite. For further verifying the effect of P, a series of bifunctional additives including spinels impregnated with different P contents were prepared. This series of aged bifunctional additives were characterized by XRD, nitrogen adsorption and Pyridine-FTIR (Supplementary data). The results indicated that the increase in the P content of spinel could slightly increase the ZSM-5 crystallinity and micropore area of the aged additives, accompanied by enhancement in Brønsted acidity.

As the number of acid sites for the aged zeolites was difficult to detect accurately only by Py-FTIR characterization at a low density level, the NH_3-TPD profiles of the aged ZSM-5 samples interacting with parent and P-modified $MgAl_2O_4$ were present in Fig. 4. It can be seen that only one desorption peak existed in all of the aged samples. The integration area of desorption curves below 300 °C

Table 4
Amount of B and L acid sites determined by FTIR of pyridine adsorption for the aged zeolites and additives at different desorption temperatures.

Sample	Total acidity (μmol g^{-1}) (200 °C)			Strong acidity (μmol g^{-1}) (350 °C)			Weak/strong
	B	L	L/B	B	L	L/B	B + L
ZSM-5	59.68	33.86	0.57	42.89	19.21	0.45	0.50
ZSM-5-M	46.25	46.26	1.00	33.67	11.12	0.33	1.07
ZSM-5-MP1	48.44	42.25	0.87	34.52	17.43	0.50	0.74
ZSM-5-MP2	50.44	46.61	0.92	34.89	22.57	0.65	0.69
K	27.12	23.66	0.87	19.67	9.77	0.50	0.73
M	23.34	27.68	1.19	15.71	13.40	0.85	0.75
M-P1	23.16	21.90	0.95	16.07	10.70	0.67	0.68
M-P2	23.88	21.75	0.91	17.58	9.20	0.52	0.70

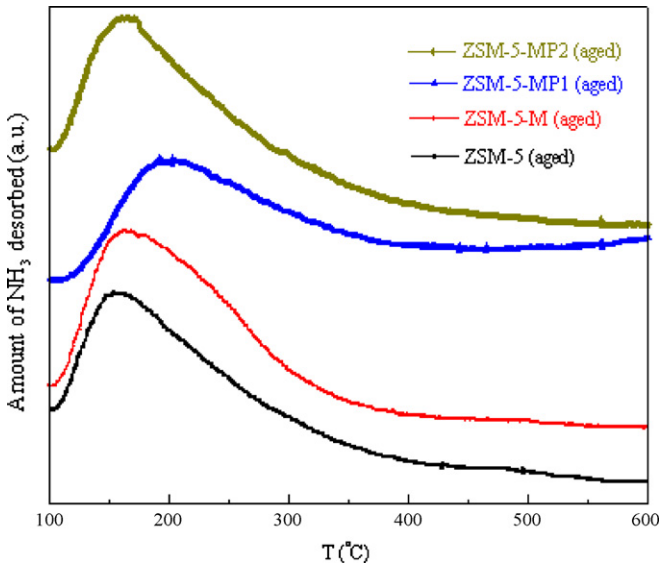

Fig. 4. NH_3-TPD profiles of the aged ZSM-5 samples.

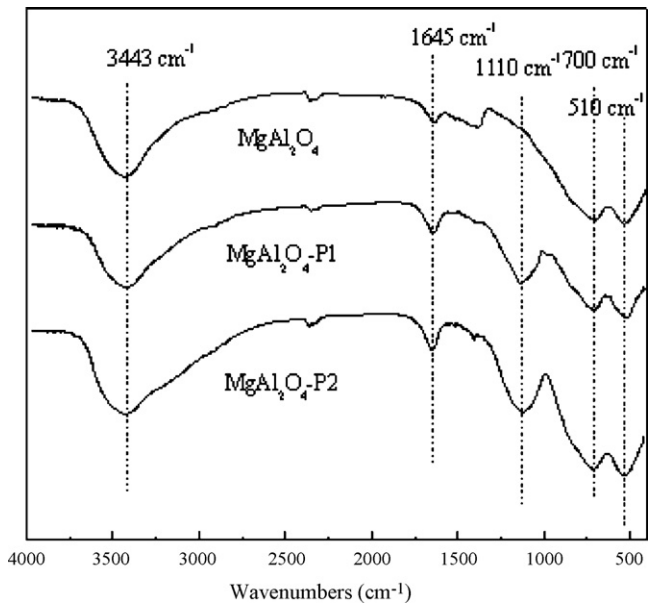

Fig. 5. FT-IR spectra of the parent and P-modified spinels.

is assigned to the weak acid amount, whereas that above 300 °C is related to the amount of strong acid sites [46]. Detailed acid amount data (not shown here) showed that the ratio of weak acid amount to the strong acid amount dramatically increased with the introduction of $MgAl_2O_4$. However, the percentage of strong acid sites greatly increased when ZSM-5 was contacted with P-modified $MgAl_2O_4$. The overall trend was accordant with that observed from Py-FTIR results. Also it should be pointed out that the change in acidity was in a larger extent when introduced P by impregnation, in conformity with the NMR results.

Additionally, the NH_3-TPD experiments of the aged ZSM-5 zeolites by direct impregnation with different contents of Mg were also carried out. The acidity calculated by NH_3-TPD profiles (Supplementary data) suggested that the acid amount decreased consecutively with increasing Mg content. More noticeably, the ratio of weak acid amount to the strong acid amount was raised as Mg content increased. However, the increase in the ratio of weak acid amount to the strong acid amount induced by the introduction of $MgAl_2O_4$ was much larger than that in the case of direct impregnation despite the lower Mg content in the former case. This could be originated by the difference in properties (especially acidity) of $MgAl_2O_4$ and MgO. But generally speaking, the effect of Mg on the ZSM-5 acidity caused by the interaction between ZSM-5 and $MgAl_2O_4$ was similar to that created by direct impregnation with Mg precursor.

Aside from the acidity, the micropore area of the additive was also an important indicator for evaluating the effect of P in stabilizing the MFI structure. For the aged additive K without the presence of $MgAl_2O_4$, the micropore area was about 115 $m^2\,g^{-1}$. And the introduction of $MgAl_2O_4$ reduced the micropore area to 69 $m^2\,g^{-1}$ for the aged additive M. However, the micropore areas of the aged additives M-P1 and M-P2 were 105 and 107 $m^2\,g^{-1}$, respectively. The results indicated that the presence of $MgAl_2O_4$ in the additives was detrimental to the microporous structure of the zeolite during steaming, whereas the introduction of P stabilized the microporous structure during the hydrothermal treatment.

Taking into account the activity ranking for VGO cracking with ZSM-5 as an FCC additive, it could be presumed that the decreased Brønsted acidity and micropore area, increased Lewis acidity and population of weak acid sites for the zeolite, orginating from the interaction of ZSM-5 with $MgAl_2O_4$, contributed to the decline in ZSM-5 activity for increasing propylene yield. While the reversion of the acidity change and restoration of the micropore area as a result of P modification should account for the higher ZSM-5 activity of M-P1 and M-P2.

3.5. *Effect of P on the properties of $MgAl_2O_4$*

As mentioned before, the initial intention of incorporating P into $MgAl_2O_4$ was to reduce the extent of interaction during steaming via suppressing the hydrolysis of $MgAl_2O_4$. The FTIR spectra of parent spinel and spinel extracted or impregnated with P recorded between 4000 and 400 cm^{-1} for checking the formation of phosphate layer were shown in Fig. 5. All of the three powders exhibited a major transmittance band at 3443 cm^{-1}, two medium bands at 510 and 700 cm^{-1}, and a minor band at 1645 cm^{-1}. The bands at 3443 cm^{-1} and 1645 cm^{-1} were associated with the –OH strechning and H–O–H bending [47], respectively. And the signals at 510 and 700 cm^{-1} were both ascribed to the streching vibration of AlO_6 groups. According to Olhero [30], the transmittance band at 1092.5 cm^{-1} for the spinel powder treated with P suggested the formation of phosphate coating on the surface of the powder. And here for the two spinel powders modified with P, the presence of a new band at 1110 cm^{-1} indicated that the phosphate coating was formed on the surface of the spinel either by impregnation or by extraction method.

In combination with the proposal that was drawn from the XRF results of zeolites, it should be deduced that the phosphate layer formed on the surface of $MgAl_2O_4$ by extraction method was more effective in suppressing the hydrolysis of $MgAl_2O_4$, resulting in the weaker interaction between $MgAl_2O_4$ and ZSM-5 during the steaming process.

Moreover, the textural and catalytic properties of P-modified $MgAl_2O_4$ would certainly be changed along with the formation of phosphate layer on the surface of $MgAl_2O_4$.

The N_2 adsorption–desorption isotherms of the aged parent and P-modified $MgAl_2O_4$ samples (not shown here) exhibited a typical mesoporous type IV isotherm shape with a H2 hysteresis loop. As seen from Table 5, the surface area and pore volume and mean pore size were all reduced by the P modification, in which the impregnation method brought about larger changes.

The performance of VGO cracking over different aged matrices was listed in Table 6 for better understanding the role of matrix in the ZSM-5 containing additives in improving propylene yield.

Table 5
Surface areas and pore properties of the aged parent and P-modified $MgAl_2O_4$ samples.

Sample	BET (m^2/g)	Micropore area (m^2/g)	Volume (cm^3/g)	Micropore volume (cm^3/g)	Mean mesopore diameter (nm)
$MgAl_2O_4$	62.33	8.19	0.217	0.0038	9.3
$MgAl_2O_4$-P1	47.88	10.43	0.144	0.0049	8.5
$MgAl_2O_4$-P2	39.45	9.90	0.124	0.0047	8.9

As to the conversion under the same C/O ratio, it decreased as the following order: Kaolin > $MgAl_2O_4$-P1 > $MgAl_2O_4$-P2 ≥ $MgAl_2O_4$. It revealed that the extraction method could evidently increase the cracking ability of spinel. Regarding the selective hydrogen transfer coefficient HTC ($(iC_4^0 + nC_4^0)/(iC_4^= + nC_4^=)$) [3,48], a markedly larger value was observed for $MgAl_2O_4$ than that for Kaolin clay. Another hydrogen-transfer indicating parameter $C_3^=$/LPG also confirmed the higher hydrogen transfer activity of $MgAl_2O_4$ than Kaolin clay. But modifying the spinel with P either by extraction or impregnation method could substantially decrease the hydrogen transfer activity. As for the non-selective hydrogen transfer activity represented by the selectivity of coke and the sum of H_2 and CH_4, $MgAl_2O_4$ was also much higher than Kaolin clay. But both of the P-modified $MgAl_2O_4$ showed remarkably lower values of coke selectivity and slightly lower values of selectivity of H_2 and CH_4 relative to the parent $MgAl_2O_4$.

When ZSM-5 is added to the FCC base catalyst, it is generally accepted that the exchange of reaction products between the base catalyst and the ZSM-5 additive is embodied in two aspects [6,7]: ZSM-5 cracks the linear olefinic products in the gasoline range produced by the base catalyst into light olefins; on the other hand, the olefins formed by ZSM-5 can be converted to paraffins by hydrogen transfer with the base catalyst. Formerly, the effects of varying cracking and hydrogen transfer activity of the base FCC catalyst on ZSM-5 performance have been investigated [3,4,12]. The effectiveness of ZSM-5 additive to enhance lighter olefins was evidently decreased by hydrogen transfer activity increment of the base cracking catalyst. But few have touched upon the effect of the matrices of propylene additives on the ZSM-5 efficiency. In this paper, as the addition amount of the ZSM-5 containing additives was low, the activity of the matrices of the additives hardly affected the cracking ability of the base catalyst. But the hydrogen transfer activity of the matrices would be influential in improving propylene yield. If the matrix of the additives holds high hydrogen transfer activity, the intimacy of ZSM-5 and matrix in the additives would confer the gasoline range olefins produced by the base catalyst and the olefins formed by ZSM-5 better chances to be saturated by hydrogen transfer reactions with the matrix of the additives.

Therefore, for the ZSM-5 containing additives, matrix with low acidity and hydrogen transfer activity is the most suitable for improving propylene yield. In this case, both the gasoline range olefins generated by the base catalyst available for the cracking of ZSM-5 and the olefins produced by ZSM-5 would be mostly retained. Thus the high hydrogen transfer activity of $MgAl_2O_4$ may probably be another reason for the decrease in the effectiveness of the additive M for enhancing propylene yield. And the decrease in the hydrogen transfer activity of spinel via P modification should also be responsible for the increased ZSM-5 activity of the bifunctional additives.

What's more, the coke selectivity is another factor that needs to be emphasized. As the lower amount of coke is formed, the blockage to the acid sites of the ZSM-5 zeolite during the reaction would be diminished, outcoming with the improvement in the efficiency of ZSM-5.

Table 6
The selective and non-selective hydrogen transfer coefficients as well as conversion of the different aged matrices for the cracking of VGO under different C/O ratios.

C/O	Catalyst			
	Kaolin	$MgAl_2O_4$	$MgAl_2O_4$-P1	$MgAl_2O_4$-P2
Conversion (wt%)				
2	20.69	17.61	21.86	17.12
3.5	32.27	24.75	30.63	26.87
5	42.96	30.74	40.75	30.80
HTC				
2	0.1485	0.3395	0.1959	0.1804
3.5	0.1727	0.3805	0.1766	0.1657
5	0.1792	0.3749	0.1421	0.1787
$C_3^=$/LPG				
2	0.3707	0.3291	0.3636	0.3600
3.5	0.3671	0.3249	0.3404	0.3617
5	0.3787	0.3274	0.3611	0.3538
Coke selectivity (%)				
2	3.77	11.81	8.05	8.71
3.5	3.97	8.48	5.22	5.32
5	3.07	8.59	4.42	3.90
$H_2 + CH_4$ selectivity (%)				
2	2.27	3.36	2.81	3.30
3.5	2.54	3.71	3.42	3.06
5	3.02	4.33	3.42	3.75

3.6. Effect of P on the adsorption activity of SO_2

Unexpectedly, treating $MgAl_2O_4$ powder with phosphoric acid through the two methods increased the uptake capacity of SO_2 in spite of the lower surface areas of the P-modified spinels than that of the parent spinel.

Some researchers suggested that the addition of P into the Al_2O_3 support, which was employed as sulfur transfer agent in FCC units, can diminish the activity loss in the alumina as a result of migration of Si from the base catalyst especially during steaming [49]. Concerning the Si poisoning, the loss of activity for sulfur-transfer agents comprised of magnesium-aluminate spinel due to Si migration from FCC catalysts during the steaming was also documented [50]. But few addressed on the direct positive effect of P on the sulfur transfer agent in eliminating SO_2. Hence the effect of P on the removal of SO_2 is not fully understood and needs to be further discussed.

The following are some explanations suggested. Firstly, the prevention of Si poisoning to the spinel owing to the presence of P may be responsible for the enhancement in SO_2 adsorption. Secondly, it can be suggestively proposed that the increased SO_2 adsorption activity may be also due to the restrain of outflow of Mg^{2+} into the zeolite. In this way, more Mg^{2+} was fixed on the surface of spinel, resulting in the promotion of SO_2 uptake capacity. And the decrease in the adsorption activity of SO_2 for M-P1-i.e. may arise from the regression in the role of P because some P species would be rinsed out during the additional ion exchange process.

4. Conclusions

When $MgAl_2O_4$ substituted for part of Kaolin clay, matrix of a typical propylene additive with ZSM-5 as the active component, the solid-state ion exchange between $MgAl_2O_4$ and ZSM-5 led to distinct decrease in Brønsted acidity. For the aged additives, the acid distribution in acid type and strength of the zeolite significantly altered and the micorpore area decreased due to the incorporation of $MgAl_2O_4$, which was mainly responsible for the decrease in the

activity of ZSM-5 as an FCC additive. Besides, the notably higher HTC value and coke selectivity of $MgAl_2O_4$ than those of Kaolin clay also contributed to the reduction in the efficiency of the bifunctional additive for increasing propylene yield.

However, the modification of $MgAl_2O_4$ with P either by extraction or by impregnation method not only inhibited the acidity change of ZSM-5 and the reduction in micropore area arisen by interacting with $MgAl_2O_4$ but also decreased the selective and non-selective hydrogen transfer activities of $MgAl_2O_4$, resulting in partial restoration of ZSM-5 activity for improving propylene yield.

Furthermore, it has been found that the introduction of P by extraction and impregnation method acted differently in weakening the interaction between ZSM-5 zeolite and $MgAl_2O_4$. The impregnation method was more helpful in restraining the interaction during calcination, whereas the phosphate layer formed on the surface of $MgAl_2O_4$ by extraction method was more effective in supressing the hydrolysis of $MgAl_2O_4$ and depressing the interaction during steaming.

On the other hand, the bifunctional additives all presented prominent effectiveness in the oxidative adsorption of SO_2. Interestingly, the P modification also had a positive impact on the removal of SO_2, possibly attributed to the restraint of silica migration during steaming and the confinement of Mg^{2+} within the matrix.

Consequently, the bifunctional additives containing P-modified$MgAl_2O_4$, which can both efficiently improve propylene yield and absorb SO_2 as FCC additives, are very promising in the future.

Acknowledgment

This work was supported by the Creation Group Foundation of the Ministry of Education of China.

Appendix A. Supplementary data

Supplementary data associated with this article can be found, in the online version, at doi:10.1016/j.molcata.2011.03.014.

References

[1] J.M. Arandes, I. Abajo, I. Fernández, M.J. Azkoiti, J. Bilbao, Ind. Eng. Chem. Res. 39 (2000) 1917–1924.
[2] C.S. Triantafillidis, N.P. Evmiridis, Ind. Eng. Chem. Res. 38 (1999) 916–927.
[3] D. Wallenstein, R.H. Harding, Appl. Catal. A: Gen. 214 (2001) 11–29.
[4] X. Zhao, T.G. Roberie, Ind. Eng. Chem. Res. 38 (1999) 3847–3853.
[5] X. Zhao, R.H. Harding, Ind. Eng. Chem. Res. 38 (1999) 3854–3859.
[6] J.S. Buchanan, Catal. Today 55 (2000) 207–212.
[7] M.A. den Hollander, M. Wissink, M. Makkee, J.A. Moulijn, Appl. Catal. A: Gen. 223 (2002) 103–119.
[8] A.A. Lappas, C.S. Triantafillidis, Z.A. Tsagrasouli, V.A. Tsiatouras, I.A. Vasalos, N.P. Evmiridis, Stud. Surf. Sci. Catal. 142 (2002) 807–814.
[9] A. Aitani, T. Yoshikawa, T. Ino, Catal. Today 60 (2000) 111–117.
[10] T.F. Degnan, G.K. Chitnis, P.H. Schipper, Micropor. Mesopor. Mater. 35–36 (2000) 245–252.
[11] J.M. Arandes, I. Torre, M.J. Azkoiti, J. Ereña, Martin Olazar, Javier Bilbao, Energy Fuels 23 (2009) 4215–4223.
[12] C. Liu, Y. Deng, Y. Pan, Y. Gu, B. Qiao, X. Gao, J. Mol. Catal. A: Chem. 215 (2004) 195–199.
[13] M.A.B. Siddiqui, A.M. Aitani, M.R. Saeed, N. Al-Yassir, S. Al-Khattaf, Fuel 90 (2011) 459–466.
[14] X. Gao, Z. Tang, H. Zhang, D. Ji, G. Lu, Z. Wang, Z. Tan, J. Mol. Catal. A: Chem. 325 (2010) 36–39.
[15] A.A. Bhattacharyya, G.M. Woltermann, J.S. Yoo, J.A. Karch, W.E. Cormier, Ind. Eng. Chem. Res. 27 (1988) 1356–1360.
[16] J.S. Yoo, A.A. Bhattacharyya, C.A. Radlowski, Ind. Eng. Chem. Res. 30 (1991) 1444–1458.
[17] J.S. Yoo, A.A. Bhattacharyya, C.A. Radlowski, Ind. Eng. Chem. Res. 31 (1992) 1252–1258.
[18] J. Wang, C. Li, Mater. Lett. 32 (1997) 223–227.
[19] J.A. Wang, L.F. Chen, R. Limas-Ballesteros, A. Montoya, J.M. Dominguez, J. Mol. Catal. A: Chem. 194 (2003) 181–193.
[20] J. Wang, C. Li, Appl. Surf. Sci. 161 (2000) 406–416.
[21] J. Wang, L. Chen, C. Li, J. Mol. Catal. A: Chem. 139 (1999) 315–323.
[22] A. Corma, A.E. Palomares, F. Rey, Appl. Catal., B 4 (1994) 29–43.
[23] A. Corma, A.E. Palomares, F. Rey, F. Márques, J. Catal. 170 (1997) 140–149.
[24] A.E. Palomares, J.M. Lópes-Nieto, F.J. Lázaro, A. Lópes, A. Corma, Appl. Catal., B 20 (1999) 257–266.
[25] C. Păcurariu, I. Lazău, Z. Ecsedi, R. Lazău, P. Barvinschi, G. Mărginean, J. Eur. Ceram. Soc. 27 (2007) 707–710.
[26] K. Prabhakaran, D.S. Patil, R. Dayal, N.M. Gokhale, S.C. Sharma, Mater. Res. Bull. 44 (2009) 613–618.
[27] J. Guo, H. Lou, H. Zhao, X. Wang, X. Zheng, Mater. Lett. 58 (2004) 1920–1923.
[28] M.J. Iqbal, S. Farooq, Mater. Sci. Eng. B 136 (2007) 140–147.
[29] X. Xu, X. Ran, Q. Cui, C. Li, H. Shan, Energy Fuels 24 (2010) 3754–3759.
[30] S.M. Olhero, I. Ganesh, P.M.C. Torres, J.M.F. Ferreira, Langmuir 24 (2008) 9525–9530.
[31] G. Jiang, L. Zhang, Z. Zhao, X. Zhou, A. Duan, C. Xu, J. Gao, Appl. Catal. A: Gen. 340 (2008) 176–182.
[32] J.Q. Zhuang, D. Ma, G. Yang, Z.M. Yan, X.C. Liu, X.M. Liu, X.W. Han, X.H. Bao, P. Xie, Z.M. Liu, J. Catal. 228 (2004) 234–242.
[33] G. Zhao, J. Teng, Z. Xie, W. Jin, W. Yang, Q. Chen, Y. Tang, J. Catal. 248 (2007) 29–37.
[34] G. Caeiro, P. Magnoux, J.M. Lopes, F. Ramôa Ribeiro, S.M.C. Menezes, A.F. Costa, H.S. Cerqueira, Appl. Catal. A: Gen. 314 (2006) 160–171.
[35] K. Damodaran, J.W. Wiench, S.M.C. Menezes, Y.L. Lam, J. Trebosc, J.P. Amoureux, M. Pruski, Micropor. Mesopor. Mater. 95 (2006) 296–305.
[36] T. Blasco, A. Corma, J. Martínez-Triguero, J. Catal. 237 (2006) 267–277.
[37] Y. Shu, D. Ma, X. Liu, X. Han, Y. Xu, X. Bao, J. Phys. Chem. B 104 (2000) 8245–8249.
[38] Y.-J. Lee, J.M. Kim, J.W. Bae, C.-H. Shin, K.-W. Jun., Fuel 88 (2009) 1915–1921.
[39] X. Li, L. Tan, C. Li, Acta Petrolei Sinica (Petrol. Proc. Sec.) 17 (2001) 57–61.
[40] M. He, Catal. Today 73 (2003) 49–55.
[41] Y.-G. Li, W.-H. Xie, S. Yong, Appl. Catal. A: Gen. 150 (1997) 231–242.
[42] J.M. Zamaro, E.E. Miró, A.V. Boix, A. Martínez-Hernández, G.A. Fuentes, Micropor. Mesopor. Mater. 129 (2010) 74–81.
[43] B. Sulikowski, J. Find, H.G. Karge, D. Herein, Zeolites 19 (1997) 395–403.
[44] S.A. Bocanegra, A.D. Ballarini, O.A. Scelza, S.R. de Miguel, Mater. Chem. Phys. 111 (2008) 534–541.
[45] J.A. Lercher, C.G. Jndling, G. Eder-Mirth, Catal. Today 27 (1996) 353–376.
[46] Y.T. Kima, K.- Jung, E.D. Park, Micropor. Mesopor. Mater. 131 (2010) 28–36.
[47] N. Phambu, Mater. Lett. 57 (2003) 2907–2913.
[48] G. Wang, C. Xu, J. Gao, Fuel Process. Technol. 89 (2008) 864–873.
[49] W.A. Blanton Jr., W. Calif, US Patent 4,243,556, 1981.
[50] R.E. Roncolatto, M.J.B. Cardoso, Y.L. Lam, M. Schmal, Ind. Eng. Chem. Res. 45 (2006) 2646–2650.